# Design Optimisation of Asciak Solar Heat Exchanger

Michael Evans PhD MIEAust

A space heating device consisting of a solar hot water heater modified for ducted airflow is analysed for optimal design variables using conventional thermodynamics and fluid mechanics theory. Prototype and specifications are copyright and patent pending of Mr Con Asciak for whom this design report has been prepared.

## *Exchanger Specifications*

The exchanger consists of a modified roof-mounted solar hot water heater with glass cover and still airspace overlying a high-emissive extruded aluminium plate and airflow chamber fed by flexible ducting. The plate incorporates extruded fins as per a conventional heat sink on its inside surface, designed to increase contact area between the circulating airflow and the heating element. The design includes a low-watt duct fan designed to assist convective movement and increase airflow or overcome resistance due to viscous friction.

The principle specifications of the design are:

1. Plate area as length and width
2. Depth of flow space underlying plate
3. Depth of extruded fins projecting into flow space
4. Extruded thickness of plate and fins
5. Optimal spacing between fins
6. Fan power and resulting optimal flowrate

Secondary specifications such as diameter of ducting and low-reflective surface coatings are incorporated and have an influence on the behaviour of the model if not necessarily the optimal settings.

Of these, items 1 and 2 are considered relatively fixed by available solar unit sizes. Item 3 is considered to be optimised by maximizing to the available flow space. Item 4 is optimised by making all plate elements as thin as possible to minimize thermal resistance.

Items 5 and 6 are considered the principle design variables and are examined in detail below.

### Fin Spacing

Fin spacing is specified by a “Fin Number”, that is the number of fins on the total width of the plate. This is an integer number that places a discrete control on fin spacing. The actual fin spacing is calculated from the fin number, plate width and fin thickness as:

Fin Spacing S = (Plate Width W– Fin Thickness t . Fin Number N)/(Fin Number N – 1)

This is the plate width less the total width occupied by fins, distributed evenly between N – 1 airflow spaces. As a check, the design program recalculates the fin number from S, W and t.

### Flow Area

Each fin blocks airspace and reduces the flow area. The working flow area is calculated as:

Working Area Aw = W . Flow Depth D – N * t * Fin Depth d

This is the total flow area reduced by the area covered by N fins each of area t . d.

### Contact Area

The contact area for convective and radiative heat exchange is increased by extruded fins projecting into the flow space. The working contact area is calculated as:

Contact Area Ac = Plate Length L . (W + N . (2 . d – t) – 2 . d)

This multiplies the overall length by the increased effective width of the plate, equal to the plate width plus N instances of 2 fin faces each of depth d. Minor corrections for the 2 outermost fin faces and for fin depths less than the flow space depth are included.

Aw and Ac are tabulated in the model with calculations of % decrease and increase.

### Exchanger Mass

N fins may add a considerable extra volume and hence weight to the extruded plate. As a check, the mass of aluminium in the exchanger is calculated by:

Mass M = 2700 . L . (W . plate thickness + N . d . t)

Aluminium is a low-density metal at 2700 kg/m3. The volume of metal is the overall length multiplied by the extruded area of the plate and fins.

## *Inflow Specifications*

The diameter of flexible ducting is specified to allow calculation of initial flow velocity and resulting inflow head losses. Inflow air temperature and pressure are estimated as 22$^{o}$C and a nominal small gauge pressure intended only to prime the system and avoid negative pressures after headloss.

Duct flow velocity is an input provided for calculation of volume flowrate in the heat exchange circuit.

Duct diameter $D_d$ = 0.25 m

Duct Flow velocity $V_d$ = 0.8 to 4.0 m/s

Duct Temperature $T_d$ = 22 $^{o}$C

Duct Pressure $P_d$ = 400 Pa = 0.058 PSI

### Inflow Thermodynamics

Total head and air density in the duct are calculated by

Duct Head $Hd = V_d^2/2g + P_d/\rho g$ as per Bernoulli's theorem

Duct Air density $\rho_d = P_d/RT_d$ as per univeral gas law

Mass and volumetric flowrates are calculated by

Mass Flowrate $m. = \rho_d . V_d . \pi D_d^2/4$ as per continuity law

Working velocity in the exchanger flow area is calculated by

Working velocity $Vw = m. / \rho Aw$

Inflow headlosses and pressure losses to the exchanger are calculated by

Inflow Headloss = $0.5Vw^2$ as per standard minor loss data

Pressure losses are calculated accordingly from the pressure-head relation $P = \rho gH$

Inflow density and temperature are calculated assuming an adiabatic or isentropic (rapid) inflow process, $P/\rho^{\gamma}$ = constant.

Generally very minor adjustments to velocity and density, with some significant pressure losses, result from these thermodynamic and fluid reaction processes.

### Reynolds Number

As the thermal conductivity and frictional resistance of air are strongly effected by turbulence, the Reynolds number is calculated for the working flow velocity and flow space dimensions of the exchanger:

$$Re = Vw \,.\, 4.\, R \,.\, \rho \,/\, \mu$$

R is the hydraulic radius of each flow space: $R = A/P = S \,.\, d/(2 \,.\, (S + d))$

$\rho / \mu$ is the kinematic viscosity of air at the working temperature

## *Environmental Variables*

The external air temperature and solar insolation rate are specified based on average midday winter design conditions, ie a typical cool sunny day optimal for performance of a solar space heater. The selected values of 13 $^{o}$C and 500 W/m$^{2}$ are based on observation of prototype performance on a given day in July 2009.

### Thermodynamic and Fluid Properties

Physical constants such as plate emissivity, specific heat and the Stefan-Boltzmann constant are given as inputs. Air viscosity is approximately constant over the working temperature range and is specified as a constant.

## *Simulation*

The model simulates the movement of an individual air package through the exchanger (a Lagrangian method), with heat exchange into the air and warming/cooling processes calculated by standard thermodynamic methods.

The air package is defined as an element of length equal to the flow velocity multiplied by a time interval of 0.01 seconds. The package moves through the system in stages equal to this time interval. In each stage the air and plate temperature are modified by heat flow into the working airflow and by re-radiation into the surrounding external environment.

This method allows calculation of plate temperatures as they vary from the inflow to the outflow of the exchanger. Thermal processes dependent on the temperature difference between the plate and the working air are thus integrated across the flow path length rather than in bulk across the total plate area.

The model does not include conduction of heat along the plate from the hotter outflow end to the cooler inflow end. This refinement was attempted, but was found to be numerically unstable with unbounded solutions and was not completed. This is not considered a drawback, since the effect of the refinement would be to raise plate temperatures at the inflow end while lowering them at the outflow end, with probably little effect on overall efficiency.

### Thermal Conduction and Heating

The exchanger consists of linked heat exchange processes:

- Absorption and re-radiation of heat by the external plate surface
- Conduction of heat through the aluminium plate and fins

- Conduction and radiation of heat into the working air flow

The thermal conductivity of air is small, but increases by a factor of approximately 10 due to turbulent mixing. A base conductivity of 0.024 W/mK is multiplied by 10 when the calculated Reynolds number exceeds a baseline of 2000. This low value is justified by the disturbance caused by entry losses into the system, resulting in a low transitional threshold.

The thermal conductivity of aluminium is much larger, 205 W/mK. As a result the system is not constrained by the transmission of heat through the aluminium, but by the slower absorption of heat into the working air. Calculations suggest a threshold to transmission constraint may occur at a fin spacing of less than 1 mm, which is outside of the construction limits of extruded aluminium.

Conduction of heat into the working air is calculated by the integral form of the heat conduction law:

$$Qc = [0.024 – 0.24] . Ac / (S / 2) . (\text{Plate Temp } Tp – \text{Working Air Temp } Tw)$$

where Ac is the contact area for an individual air package, equal to the effective plate width times the element length. The minimised thermal resistance S/2Ac reflects the increase in contact area and the decrease in conductive path length due to fin spacing.

Radiation into the working air is calculated using the Stefan-Boltzmann law:

$$Qr = e . Ac . \sigma . (Tp^4 – Tw^4)$$

where e is the emissivity of the inside surface of the plate (~ 0.9 for black aluminium) and $\sigma$ is the Stefan-Boltzmann constant, 5.67 x10-8 $W/m^2K^4$

The total air heating rate is the sum $Q = Qc + Qr$

A total heat input in each time increment is calculated by the heating rate times the time interval, $\Delta Q = Q . \Delta t$

The working air temperature change due to heat input is calculated from the heat capacity law:

$$\Delta Q = m . Cp . \Delta T$$

where m is the mass of the air element, Cp is the specific heat of air = 1005 J/kgK and $\Delta T$ is the temperature change. In each time interval the heat input produces a temperature increment which is added to the working temperature for the next time step:

$$\Delta T = \Delta Q / ( m . Cp )$$

The plate temperature at each increment is then calculated by considering the re-radiation potential of the plate. Heat absorption into the working air is subtracted from insolation into each increment of plate, giving a net re-radiation from the plate:

$$e . \text{Insolation} – \Delta Q = \text{re-radiation } Qre$$

where e is the external plate emissivity and insolation is the thermal energy arriving at each plate element in the time interval:

$$\text{Insolation} = \text{Environmental Insolation [~ 500 W/m2]} . \text{Element Plate Area } Ap . \Delta t$$

The element plate area is the length of the element length multiplied by the plate width

$$Ap = Vw . \Delta t . W$$

The repeated $\Delta t$ term arises due to the use of a natural length unit for the simulation.

The re-radiation from the plate is governed by the Stefan-Boltzmann law, by which the plate interacts with the external environmental temperature:

$$Qre = e \,.\, Ap \,.\, \sigma \,.\, (Tp^4 - Te^4)$$

This can be manipulated to isolate Tp as a unique function of the preceding calculations:

$$Tp = ( Qre / (e \,.\, Ap \,.\, \sigma) + Te^4)^{1/4}$$

## Viscous Friction

Reynolds number depends on the fin spacing, a key variable in the hydraulic radius of each flow space, having the effect of constraining turbulent motion. A friction factor is calculated as a function of Reynolds number, using two ranges:

| | | |
|---|---|---|
| $Re < 2000$: | $f = 64/Re$ | (Reynolds) |
| $Re > 2000$: | $f = 0.316/Re^{0.25}$ | (Blasius) |

Reynolds numbers were not found to exceed a value of 10,000 where the more complex Colebrook-White formula is required.

Friction headloss is calculated using the Darcy-Wesibach equation:

$$Hf = f \,.\, L \,.\, Vw^2 / (8 \,.\, g \,.\, R)$$

Where L is the natural element length, Vw is the working velocity and R is the hydraulic radius within a flow space.

Pressure losses are simulated from headlosses by the pressure-head relation $\Delta P = \rho g \Delta H$

## Thermal Expansion and Acceleration

A polytropic heating process is simulated by thermal expansion, using a compressible expansion coefficient

$$B = 1/Tw$$

where Tw is the working temperature in Kelvin. Expansion and acceleration were found not to be significant variables in this low speed environment, but were retained for completeness.

## Exchanger Residence Time

The time each working air element spends in the exchanger is proportional to the total energy absorbed: higher flowrates reduce the residence time and may reduce the net heat flow depending on the total balance of thermal and loss-making variables. The residence time is calculated by summing time intervals where the sum of element lengths is equal to the path length of the exchanger. This is reported as a variable, but has no further role in calculations, since heat inflow is simulated by integral rather than bulk methods.

## Space Heating

The output from the simulation consists of a mass flow rate, solar energy input rate and an outflow working air temperature To. This enables calculation of circulation time within the house side of the thermal circuit, allowing timed cooling of the working air and the development of temperature distributions within the house.

The circulation time is calculated by

$$tc = V / Q$$

where V is the volume of the house and Q is the volume flow rate. Cooling is achieved by Newton's law using a thermal coefficient derived from conductivity, capacity and surface are of the house:

$$Ti = Te + (To - Te) \,.\, e^{-r \,.\, tc}$$

where r is a constant r = hA/Cp, h equal to the laminar thermal conductivity of air and A the surface area of the house. This was adjusted to suit the system so that cooled air temperatures were in a reasonable range as per observations in Winter 2009.

An average temperature based on the mean of To and the cooled inflow Temperature Ti is calculated. This average temperature should ideally consist of consistent moderate outflow and inflow temperatures rather than distinct hot and cold areas in different parts of the house. This may arise for example where the mass flow rate is too low, giving too much residence time and an overheated working fluid, coupled with too much circulation time and a pronounced cooling on the house side. This condition is explored further below.

A mean energy density is calculated from the solar input rate and the mass flow rate:

$\rho e = Q / m.$ units J/kg.

Since the flowrate tends to decreases more rapidly than the corresponding solar input rate it appears that energy density increases with decreasing flowrate, however this may be a useless trend, since even if a large energy is stored in each kilogram of air, insufficient air mass may pass through the system to maintain the house temperature. The average Temperature calculated above is considered a more reliable measure of the optimal effectiveness of the heating system.

### Fan Power

The system is powered by a house fan or similar low-watt device. The fan power is calculated by the mass flow rate and total headloss through the circuit:

Fan Power $Pf = \rho . g . Q . \Delta H$

It is found that the fan power increases incrementally with marked thresholds at the transition from laminar to turbulent. Fan power is essential for the operation of the system and is factored into efficiency calculations.

### Solar and Total Efficiency

The solar efficiency of the exchanger is calculated as the ratio of total heat input rate across the flow path length to the solar insolation rate:

Efficiency $\zeta = Q / I$

The total efficiency subtracts the power required to operate the fan. This is an essential component of the efficiency, since high flow rates are associated with high friction and minor losses that reduce the overall efficiency. As a result, fan operation and fin spacing are limited to values within a low decompression range.

Total Efficiency $\zeta = ( Q – Pf ) / I$

## *Optimisation*

The model as described was run for a range of design variables including:

- plate and fin thickness
- fin depth and spacing
- internal and external emissivity
- flowrate

A series of composite graphs were produced showing output variables for the key design variables of flowrate and fin spacing. These are outlined in the following pages.

## Flowrate Variables

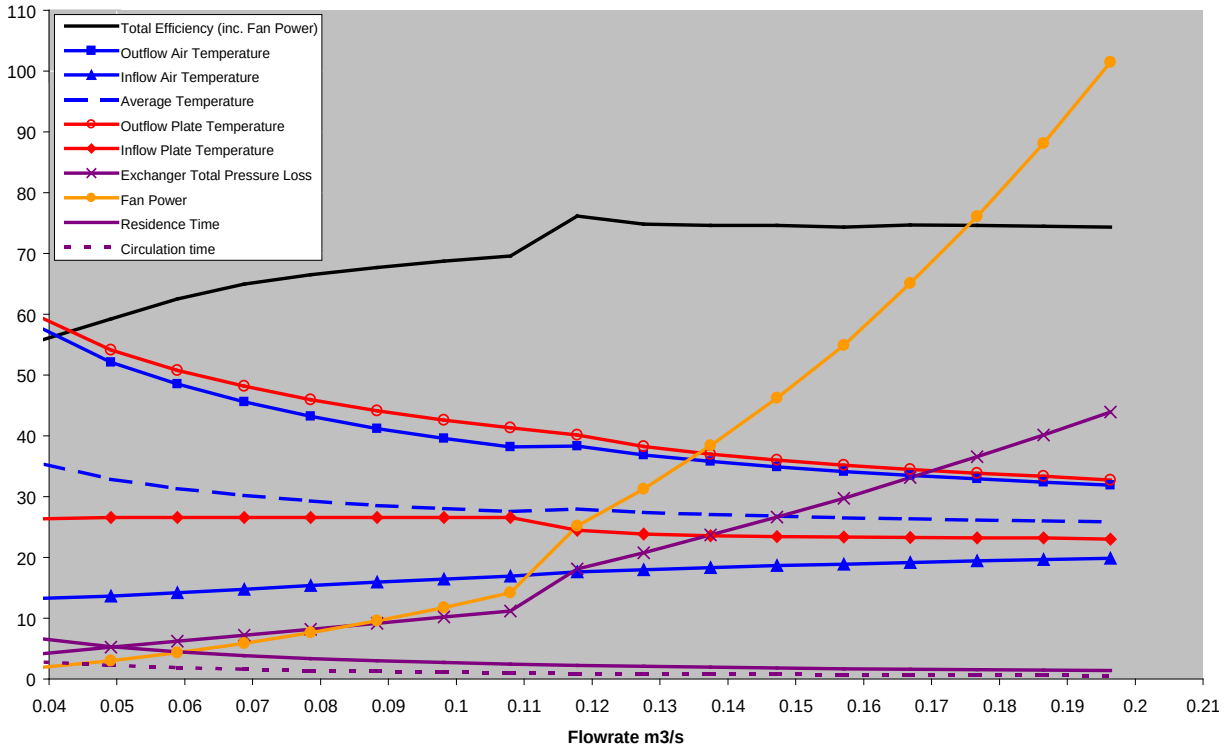


The composite shows a number of trends and a significant threshold effect around the onset of transitional turbulence. For flowrates greater than around 0.12 $m^3/s$ the total efficiency is effectively constant or falling slightly, possibly with more than one optimal point. Over most of the range tested the working fluid outflow temperature matches the outflow plate temperature, which falls as the increasing mass flowrate improves the removal of heat from the plate.

For low flowrates the combination of high residence times (a few seconds) and high circulation times (a few hours) leads to large temperature changes both within the exchanger (heating) and within the house (cooling). As a result the average temperature is high and based on a wide temperature range in different parts of the house. This is undesirable, as described above.

Low flow rates are also associated with high plate temperatures, since there is insufficient mass flow of working fluid to extract heat from the plate. As a result the plate re-radiates large amounts of heat, leading to a low total efficiency despite the almost negligible losses to friction and fan power.

The laminar-turbulent transition occurs at around 0.11 to 0.12 $m^3/s$, with associated step changes in thermal and fluid processes. A pronounced increase in heat absorption due to higher thermal conductivity of turbulent air leads to a steepening of the plate temperature curve. The rapid increase in fan power above this point becomes the dominant influence on the efficiency curve, which would otherwise continue to rise with increasing absorption (due to increased contact area and diffusive conduction) and reduced re-radiation.

The peak efficiency appears to coincide with an inflection of the average temperature, above which average temperature does not change much even as inflow and outflow temperatures converge.

120 litres/s is highlighted as a point of best efficiency and a range in which space heating output is both moderate and uniform.

## Fin Number Variables

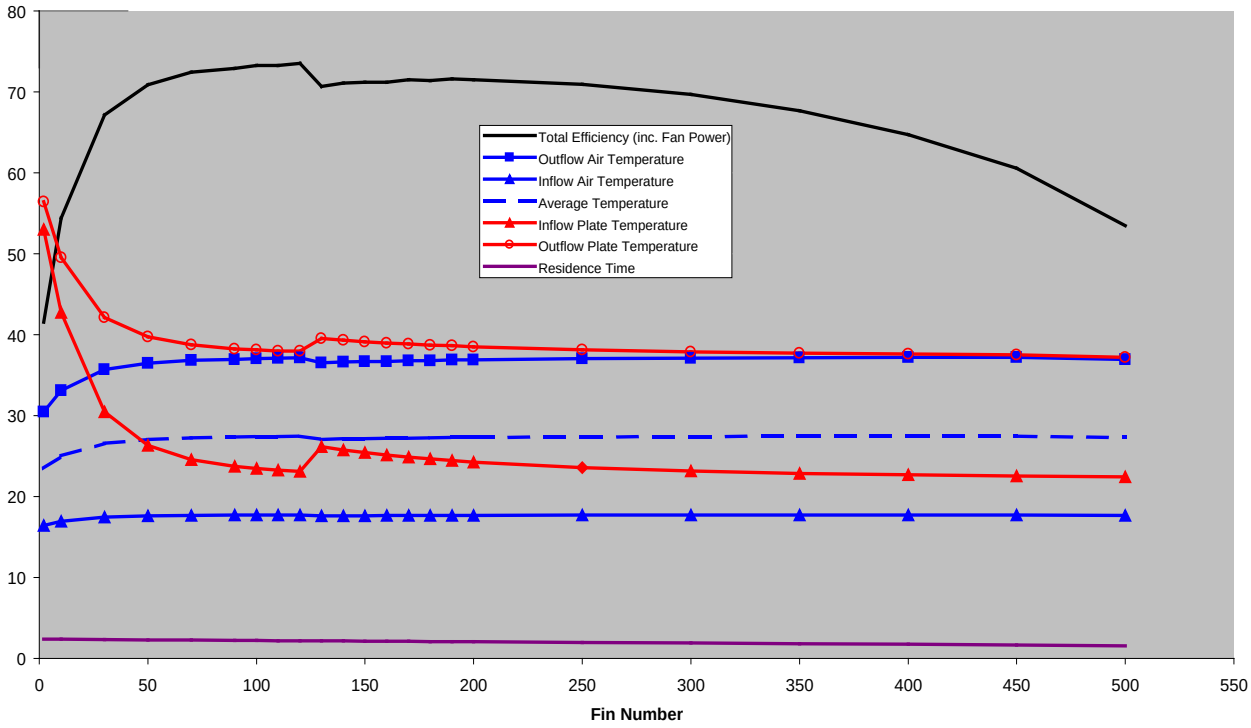


The composite shows a more pronounced trend in plate temperatures and a different trend in working fluid temperatures to that of the flowrate composite. Again the point of best efficiency coincides with the onset of turbulence, which occurs as the fin number falls below about 120, or fin spacing greater than 11 mm.

For low fin numbers the transmission of heat into the working fluid is inefficient, with the result that the plate temperature at inflow and outflow are high. As fin number increases the contact area and absorption increase, cooling the plate and increasing the efficiency. The inflow end of the plate is more effectively cooled since it is in contact with cooler inflow air.

Lower plate temperatures indicate less radiative heat loss from the plate and correspondingly higher absorption and outflow temperatures in the working fluid. The average temperature on the house side of the circuit approaches a maximum of about $27^{o}$ at around fin number 50.

The laminar-turbulent transition occurs at about 120 fins per 1.5 m width, becoming laminar with increasing fin number. Laminar flow is assumed to onset below a Reynolds number of 2000, reducing the thermal conductivity of the working fluid and so reducing absorption. Re-radiation increases with a step increase in plate temperature and decrease in efficiency and outflow temperature.

**The efficiency appears to be limited by the convergence of the outflow and plate temperatures at around $37^{o}$. Improving the design may depend on limiting the gain in outflow temperature so that the convergence happens at a lower plate temperature with corresponding higher efficiency.**

The model is not sufficiently rigorous in the modeling of turbulence to locate the optima with precision. Turbulence remains a poorly understood phenomenon, with limited success in even full 3D solutions, which this model does not attempt. Better estimates of this point will derive from experimental or prototype observations rather than theoretical modeling.

A fin number of 120 is highlighted as a point of best theoretical efficiency just before the onset of laminar flow. This corresponds to a fin spacing of 11.6 mm. Maintaining or increasing turbulence by surface roughening beyond this point is unlikely to improve efficiency. The optima may be somewhat less than N = 120 due to the plateau of near-optima from 50 to 100.

## Constraints

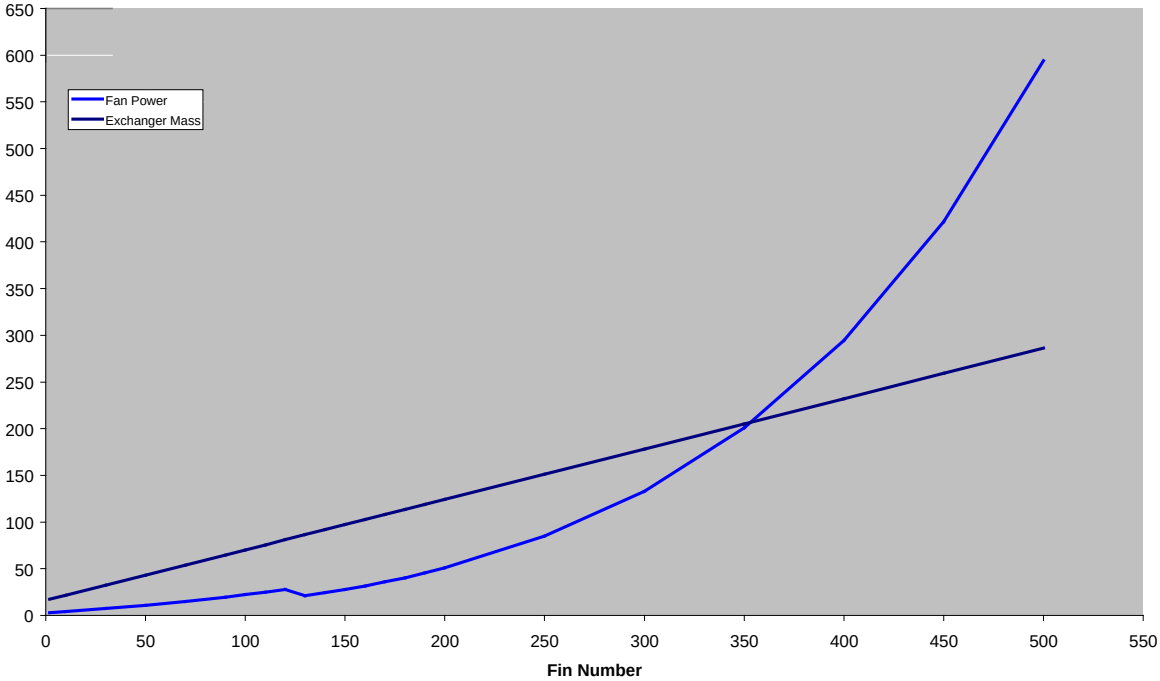


At fin numbers above 200 the headloss in the system becomes significant, with an exponential increase in fan power and reduced overall efficiency. Fan power shows a typical system curve with increasing headloss for decreasing hydraulic radius, including a minor step down at the turbulent-laminar transition. This is in contrast to the step up seen in the flowrate variables, where the transition is from laminar to turbulent. The step seen here is due to the change in friction factor from Blasius to Reynolds regimes in the Moody diagram.

Another significant constraint is the mass of the exchanger, which increases from 17 kg total with no fins to about 100 kg at fin number 150. While target variables such as efficiency and average house temperature plateau between fin numbers 50 to 100, the exchanger mass continues to increase as a linear function of N. This will increase handling and transportation costs and should be taken into account when selecting the optima.

## *Sensitivity Testing*

The graphs of fin number and flowrate variables are centred on an optimal intersection: Fin number is held at 120 while flowrate is varied, and flowrate is held at 0.120 m3/s while fin number is varied. This is a “first cut” dissection of system performance.

Subsequent sensitivity testing is intended to position the optima for higher and lower intersections, and as a means to further explore system performance.

### High Flow Rate

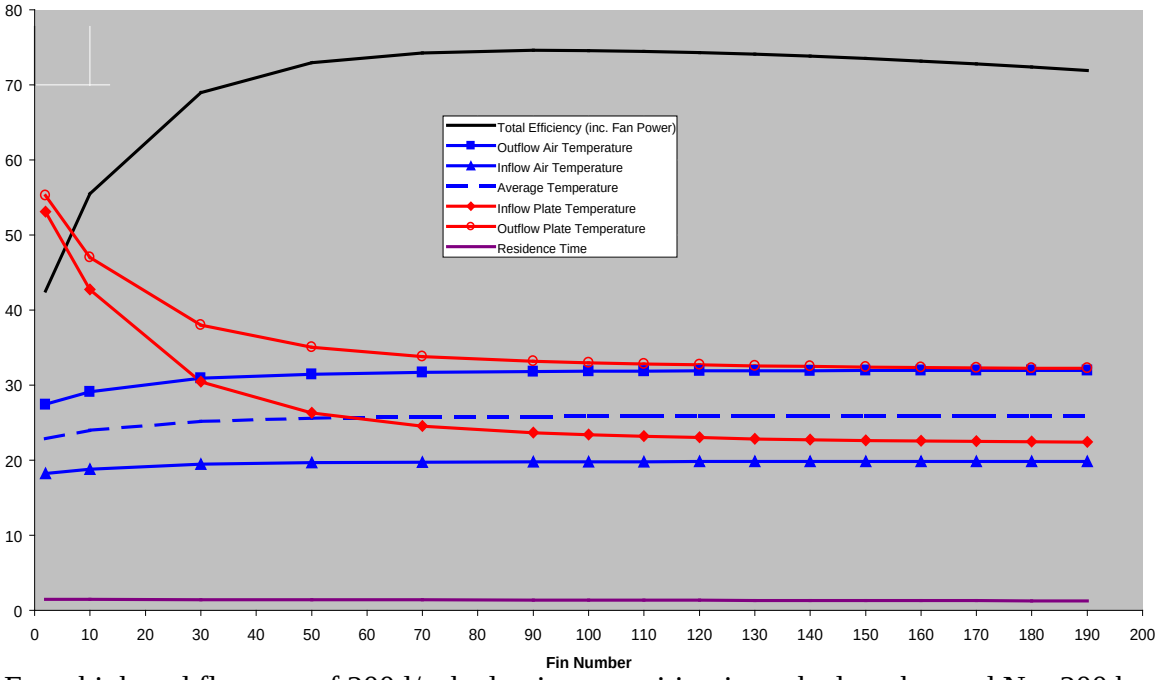


For a high end flowrate of 200 l/s the laminar transition is pushed out beyond N = 200 by the increase in flow velocity. In this range the laminar transition is no longer a constraint.

Plate temperatures are cooler due to the increased mass flowrate. Since this results in lower re-radiation the overall efficiency is slightly improved. Efficiency is again constrained by the convergence of plate and outflow temperatures at around $33^{o}$, the lower convergence corresponding to lower re-radiation and higher efficiency .

Fan power becomes more significant as a factor reducing overall efficiency.

Average house temperature is slightly reduced with a small overall range due to reduced circulation time and cooler outflow temperatures.

Fan power (not shown here) increases more quickly than for the mid-range “optimal” flowrate setting, but is less than 100 W for the optimal point and is not a serious constraint.

Optimal fin number has shifted back slightly to around N = 100, about 14 mm spacing. Lower values down to N = 70 are at nearly the same performance within a broad plateau.

## Low Flow Rate

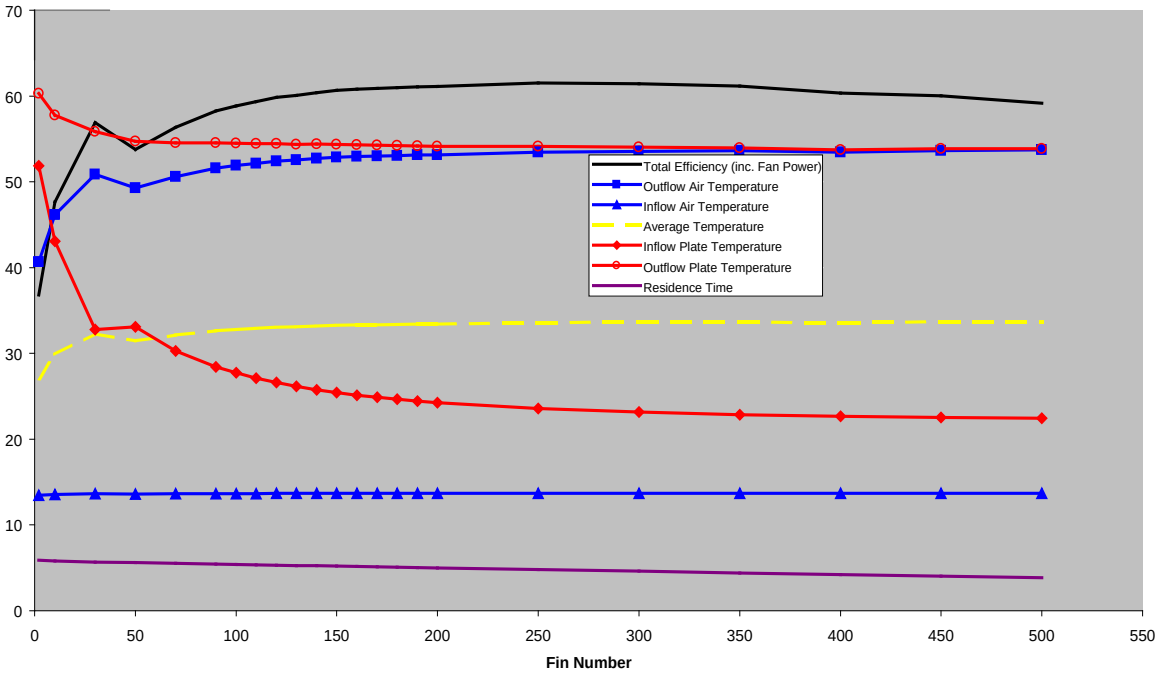


For a low end flowrate of 50 l/s the laminar transition is brought back to around N = 30 with a corresponding step in performance. Efficiency recovers significantly, an effect not seen in the high and mid-range flowrates, but never goes much past a significantly poorer 60%.

Efficiency is again constrained by the convergence of plate and outflow temperatures, this time at a much higher temperature around 54$^{o}$. The higher temperature is due to long residence times in the exchanger. Average house temperatures are overly warm with very serious hot and cold areas appearing in the house due to long circulation times. Outflow air is overheated by long exposure to the plate, and return air has all but cooled to the external ambient temperature.

Optimal fin number has increased to around 250 corresponding to an exchanger mass of 150 kg.

Overall the low flowrate system does not appear to be competitive with mid-range or high.

The comparison suggests that higher flowrates should be further investigated.

## Overdrive

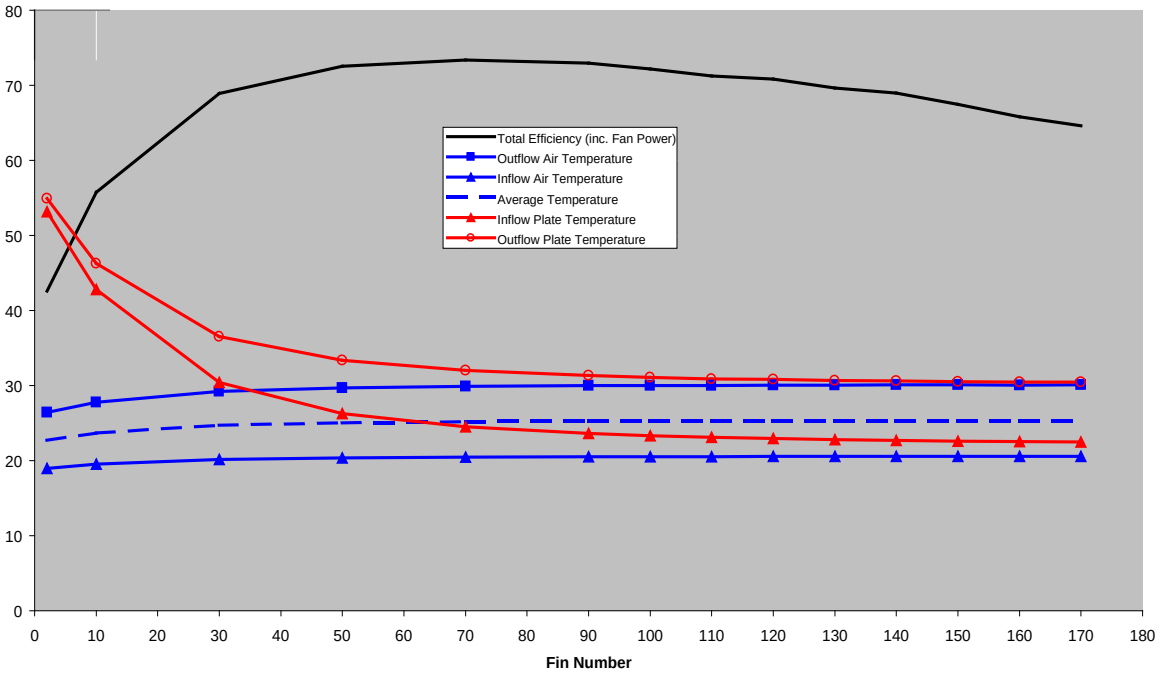


At an overdriven flowrate of 250 l/s the convergent plate-outflow temperature is reduced still further, but efficiency gains are eroded by the increase in fan power required. Optimal fin number is again lower at around N= 70. Efficiency is slightly less than for the 200 l/s high flowrate.

This suggests a search for optima around 200 l/s and N = 70 to 100.

A maxima of 74.8% was found in the efficiency curve at (Q, N) = (182 l/s, 100). A detail view of the flowrate variable around this range indicates a complex multi-modal behaviour of the efficiency curve, suggesting very close competition between trends. There is no single optima.

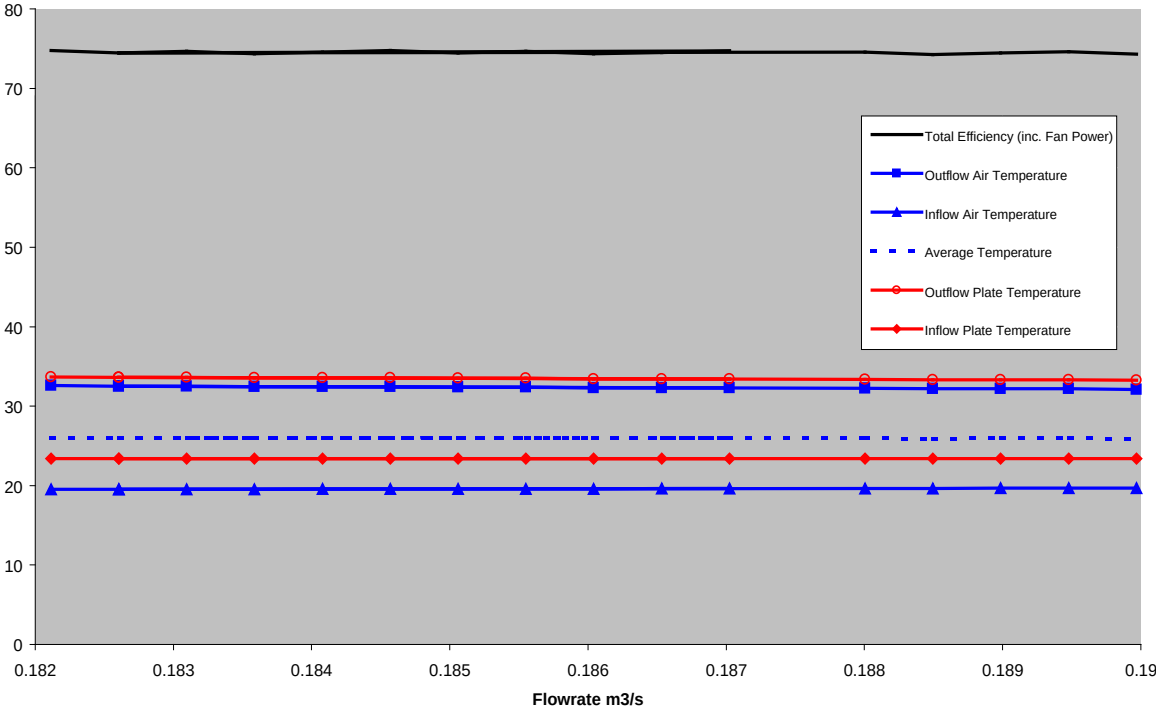

## *Design Alternatives*

Consultation and model discussion with the patent holder resulted in identification of a significant improvement in the design: a re-orientation of 90$^{o}$ so that the smaller dimension of the exchanger becomes the flow path length rather than the width, while the former width becomes the length. In construction terms this amounts to orienting the fins and ducted flow *across* rather than *down* the panel.

Two consequences of this modification are a shorter flowpath and a wider flow area, both of which represent a reduction of head loss within the exchanger. The resulting optimal total efficiency increases from around 74.5% to around 78.5%. This point occurs at flowrate 187 l/s and fin number 115, or 16.5 mm fin spacing. Optimal performance graphs are shown below.

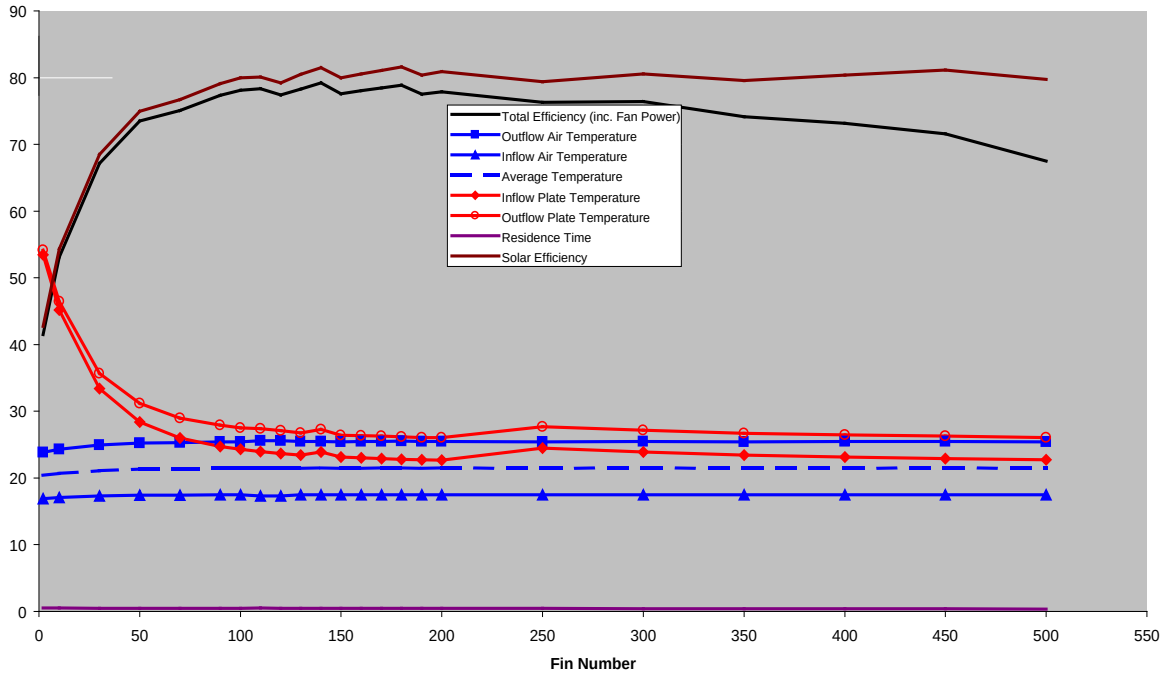


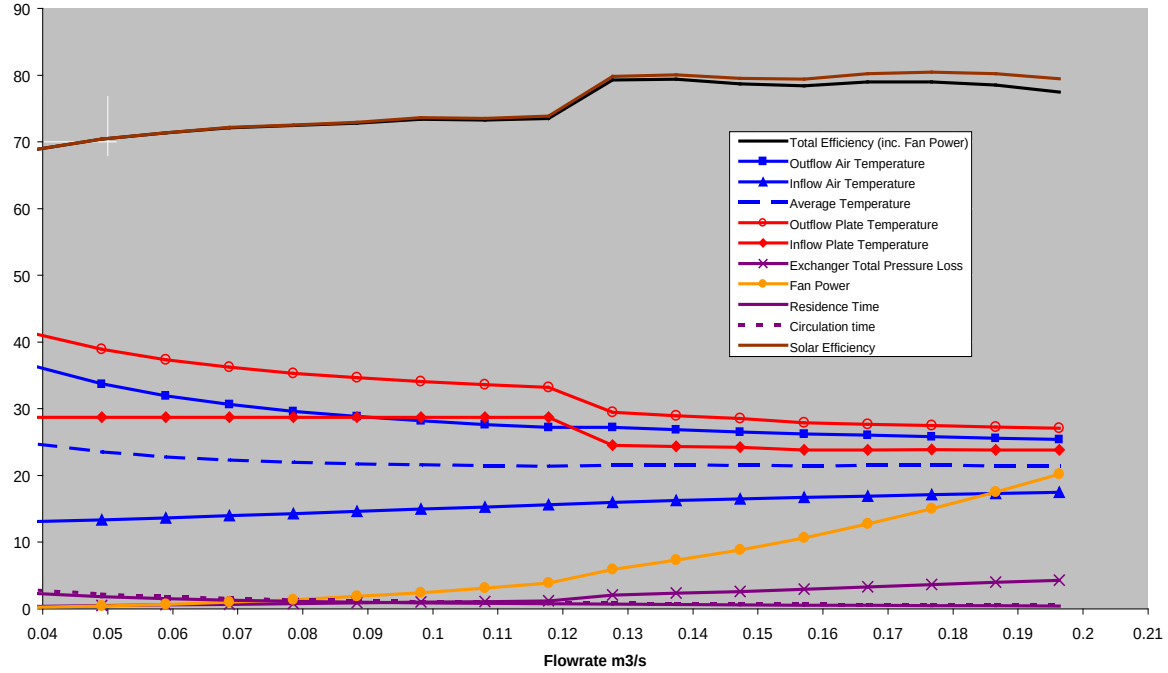

## *Revised Constraints*

Fan power calculations were subsequently modified to include head losses within duct lines, at wall inlets and outlets, and within the house itself. House losses are negligible, however losses in the hydraulically rough flexible ducting and inlet/outlets are significant and result in downwards adjustments of total efficiency.

The weight constraint was adjusted by defining the proposed commercial size of units as 2 x 1 m, rather than 2 x 4 as per the prototype's two units in series. This large reduction in area results in a smaller calculated mass for any fin spacing and thickness. A unit of dimensions 1 x 2 $m^2$ and 16.5 mm fin spacing weighs 20.9 kg, comparable to a standard gyprock wall panel and easily managed by a team of two construction workers with appropriate roof lifting gear.

## *Recommendations*

It is recommended that a prototype solar exchanger be constructed to the following specifications:

1. Maximise plate area as length and width (1 x 2 m)
2. Orient flowpath to the smaller dimension of the exchanger (flowpath length = 1 m)
3. Maximise depth of flow space underlying plate (50 mm)
4. Maximise depth of extruded fins projecting into flow space (50 mm)
5. *Minimise* extruded thickness of plate and fins (1 mm)
6. **Optimal spacing between fins is estimated as 16.5 mm**
7. **Optimal flowrate is estimated as 187 l/s.**

Fan power specifications in this design are indicative or comparative only, and are subject to prototype performance testing. The model incorporates significant loss terms through the entire circuit, however loss factors are uncertain and approximately estimated, hence the optimal fan power may differ significantly from that modelled here.

## References

All theoretical materials used in the development of the model and preparation of the report are standard fluid mechanics and thermodynamics textbook theory.

## Acknowledgements.

Thanks to Mr Ken MacDonald, consulting metallurgist, who provided additional insights into the thermodynamics of extruded metal surfaces and confirmed the application of the theoretical plate heating and cooling material in the model.